Measurement of the $2S$ atomic hydrogen hyperfine interval

N. E. Rothery and E. A. Hessels
York University, 4700 Keele Street, Toronto, Ontario, Canada M3J 1P3
(Received 28 October 1999; published 1 March 2000)

The $n=2S$ metastable-state hyperfine interval in atomic hydrogen has been measured to a precision of 160 ppb by driving the magnetic-dipole radio-frequency transition in a thermal beam. The $2S$ hyperfine interval is found to be $177\,556\,785\pm29$ Hz which is the most precise measurement of this interval.

PACS number(s): 32.10.Fn, 32.30.Bv

One of the most precisely measured quantities in physics is the hyperfine structure of the ground state of atomic hydrogen [1], which is known to one part in 10^{14}. This measurement poses a strong test of theory in the simple one-electron system. However, theory [2] in this system is limited to a precision of one part per million due to the uncertainty in the structure of the proton.

In the present work we measure the $2S_{1/2}F=1m_F=0$ to $2S_{1/2}F=0m_F=0$ hyperfine interval of atomic hydrogen. The only previous measurement of the $2S$ hyperfine interval was done in 1956 by Heberle, Reich, and Kusch [3], who measured the interval to be $177\,556\,860\pm50$ Hz. The present measurement has achieved a precision of 160 ppb with a measured $2S$ hyperfine interval of $177\,556\,785\pm29$ Hz. This measurement represents the most precise measurement of the $2S$ hyperfine interval to date.

The hyperfine intervals depend on both proton structure and quantum electrodynamic effects. By taking a linear combination of the very precisely measured $1S$ and $2S$ hyperfine intervals, it may be possible to remove proton structure effects allowing for a test of purely quantum-electrodynamic contributions.

The $2S$ hyperfine interval in atomic hydrogen is measured using an atomic beam apparatus shown schematically in Fig. 1. A thermal beam of atomic hydrogen is created by allowing a small flow of molecular hydrogen to pass though a palladium leak valve into a rf dissociation region [4,5] which consists of an air-cooled Pyrex tube surrounded by a rf buildup cavity. The cavity [6] is driven with 50 W of 47-MHz rf radiation, and, with 1 Torr of hydrogen in the Pyrex discharge tube, a plasma is created that dissociates hydrogen molecules with an efficiency of 90%. The hydrogen atoms thus produced are allowed to flow through a short Teflon tube to the electron bombardment region [7]. In this region the beam of atomic hydrogen crosses a beam of 11-eV electrons at an angle of intersection of 110° (See Fig. 1).

The electron beam is prepared by heating a thoriated tungsten filament. The electrons are accelerated through a grid (which is biased by 11 V relative to the filament) toward the atomic hydrogen beam. A magnetic field of 575 G helps to collimate the 10-mA electron beam. Collisions between the electrons and the hydrogen atoms produce excited states of atomic hydrogen including $2S_{1/2}$ metastable states. At thermal speeds, only the long-lived (0.12 s) $2S_{1/2}$ state survives for the average 40-ms time that it takes for the atoms to travel to the next part of the experiment. The electron collisions deflect the excited hydrogen atoms by approximately 20°. The 575-G field mixes the $2S_{1/2}F=0m_F=0$ and $F=1m_F=-1$ states with short-lived (1.6 ns) $2P_{1/2}$ states [3]. This mixing causes the population in these two states to decay quickly to the ground state, and thus the $2S_{1/2}$ atoms which exit the electron bombardment region are primarily in the $2S_{1/2}F=1m_F=0$ and $2S_{1/2}F=1m_F=+1$ states.

After the electron bombardment region, the $2S_{1/2}$ atoms enter the main rf interaction region. This region is composed of a 98-cm-long transmission line which transmits 177-MHz radio waves. It is a 50-Ω transmission line constructed out of WR430 (4.30×2.15 in.) copper waveguide with a 1.125-in.-outer-diameter round inner conductor. The region is engineered to have very low rf reflections ($|\Gamma|<0.03$). It is the rf magnetic field of these waves which is used to transfer population from the $2S_{1/2}F=1m_F=0$ state to the previously emptied $2S_{1/2}F=0m_F=0$ state. The frequency of the radio waves is scanned in a systematic fashion over the hyperfine resonance in order to determine the center of the resonance. A dc magnetic field of 22, 34, 53, 83, or 119 mG is applied in the main rf region to ensure that only the $m_F=0$ to $m_F=0$ transition is driven.

When the metastable atoms exit the main rf region they enter another rf region in which 40-mW 900-MHz radio waves are used to transfer newly created $2S_{1/2}F=0m_F=0$ atoms to the short-lived $2P_{1/2}F=1m_F=0$ state, thus effectively removing the $2S_{1/2}F=0m_F=0$ population. The remaining metastable atoms move into a large-solid-angle Lyman-α detector [8]. Inside the detector, an electric field of about 2 V/cm is applied, which is sufficient to mix the $2S_{1/2}$ states with $2P_{1/2}$ states. The 2-V/cm field causes $2S_{1/2}$ atoms in the detector to quickly decay to the ground state by emitting a Lyman-α photon at 121 nm. The 121-nm photon is detected upon entering a NO detector, where it ionizes a NO molecule with 80% efficiency. The resulting electrons are collected and preamplified, and the resulting signal sent to a

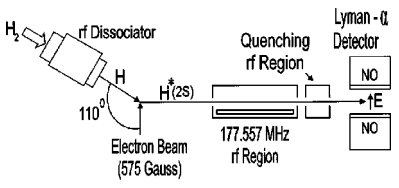

FIG. 1. Schematic diagram of the experimental apparatus. Details of the experiment are described in the text.

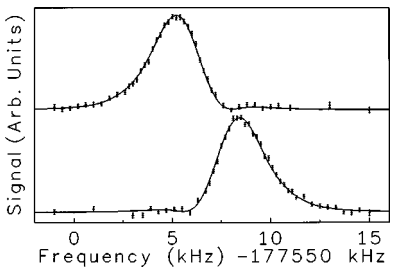

FIG. 2. Average of data taken with an applied dc magnetic field of 53 mG. The bottom curve represents the data taken with the rf propagating in the same direction as the atoms. The top curve represents data taken with the rf propagating in the opposite direction from the atomic beam. The error bars shown represent one standard deviation uncertainties.

lock-in amplifier. The lock-in amplifier detects the signal synchronous with 100% amplitude modulation of the radio waves sent to the main rf interaction region.

When the radio waves are off resonance, both $2S_{1/2}F=1m_F=1$ and $2S_{1/2}F=0m_F=0$ atoms arrive at the detector, whereas, when the radio waves are on resonance, only the atoms originally in the $2S_{1/2}F=1m_F=+1$ state are detected. From the lock-in amplifier output signal versus applied rf frequency one obtains a scan of the line shape of the $2S_{1/2}F=1m_F=0$ to $2S_{1/2}F=0m_F=0$ resonance (see Fig. 2). Many such scans are taken (approximately 1000 h of data) while varying a variety of experimental parameters, and they are used to determine the $2S$ hyperfine interval to very high precision.

The largest systematic shift in the $2S$ hyperfine interval is due to the Doppler shift. Thermal metastable atoms move at velocities of approximately 2600 m/s, and the radio waves used to excite them are traveling either copropagating or antipropagating with the atoms. The resulting Doppler shift ($\Delta\nu_D=\beta\nu$) is $+1.5$ and -1.5 kHz for the two propagation directions. Throughout this experiment, copropagating and antipropagating data are always taken in succession, with all other experimental parameters remaining fixed.

From time-dependent perturbation theory, the expected lineshape for an atom spending a time τ in the rf field is

$$S(v)=4V^2\left(\frac{\sin(\pi\Delta\tau)}{\Delta}\right)^2, \tag{1}$$

where $\Delta=\nu-\nu_O'$ and $\nu_O'=\nu_O\pm\beta\nu$. Here ν is the frequency of the applied radio waves, ν_O is the center of the hyperfine interval, $\beta=v/c$, v is the speed of the metastable hydrogen atoms, $\tau=L/v$ is the length of time the atoms spend in the $L=98$ cm main rf interaction region, $V=\mu_B B/2h$, μ_B is the Bohr magneton, and B is the amplitude of the rf magnetic field.

The speed distribution of thermal atoms moving out of a small hole is [9]

$$P(v)\propto U^3e^{-u^2}, \tag{2}$$

where $U=v/\alpha_T$, $\alpha_T=(2kT/M)^{1/2}$, k is the Boltzman constant, T is the temperature of the atoms, and M is the atomic mass.

Our best estimate of the speed distribution actually found in our atomic beam and contributing to our resonance is the distribution of Eq. (2), with a speed cutoff which excludes atoms under a certain speed ($v_{\min}$). These slow-moving atoms are deflected by too large an angle by the electron collisions, and thus are not directed down our beam line. Slower atoms also spend too much time in the fields present in the electron-bombardment region, and thus tend to mix with the $2P$ state and decay down to the $1S$ state. A third reason for excluding slow-speed atoms is that these atoms tend to decay down to the ground state too early in the detection region, causing a lower efficiency for detecting the Lyman-α photon.

The expected line shape is obtained by integrating Eq. (1) over the expected speed distribution in the metastable beam:

$$S(v)=\int_{v_{\min}}^{\infty} CU^3e^{-u^2}4V^2\left(\frac{\sin(\pi\Delta\tau)}{\Delta}\right)^2 d\nu+D. \tag{3}$$

Figure 2 shows data fit to this line shape. In this fit, the height C, the offset D, the center ν_o, the cutoff $v_{\min}$, and α_T are all floated.

As expected, the offset parameter D is consistent with zero for all fits. The $v_{\min}$ values are near 2000 m/s, indicating that the lowest 15% of the thermal-beam speed distribution does not contribute to the resonance. If, in addition, we float L (the length of the main rf interaction region), the fit parameters are consistent with the 98-cm physical length of the main rf interaction region, except for the case of the 34-mG data. The 34-mG data are taken with a very nonuniform magnetic field, and the 70 ± 1-cm length returned by the fit corresponds approximately to the distance over which the magnetic field is uniform in the vertical direction. Only a small portion of the data is taken at this magnetic field. The α_T values are near 2600 m/s, corresponding to a temperature of 410 K, which is consistent with that expected in the H_2 discharge based on previous studies [5].

The effect of the Doppler shift and the velocity distribution is to shift the resonance and to make it asymmetric. Data taken with the two different rf propagation directions have opposite shifts and asymmetries (as shown in Fig. 2). The first-order Doppler shift exactly cancels when the average of the two centers is taken. This average center is also found to be very independent of the line shape used for the fitting, with line shapes as poor as symmetric Lorentzians giving almost identical average centers.

A small portion of the rf field reflects from the ends of the rf region. Thus, when the main rf field is copropagating with respect to the atoms, a small reflected rf field is antipropagating with respect to the atoms. The effect of the antipropagating reflected wave has been modeled [10] using time-dependent perturbation theory, and is found to lead to a shift of less than 11 Hz. By physically reversing the orientation of the rf region, the sign of this shift changes. We see a difference of -8.2 ± 16.3 Hz for the two orientations of the rf

TABLE I. Summary of fit centers, systematic corrections, and final results. Column 1 shows the dc magnetic field present in the main rf interaction region. Column 2 lists the average fit centers for each magnetic field. Column 3 shows the shift due to the dc magnetic field. Column 4 lists the fit centers corrected for the dc magnetic-field shift. The weighted average of these corrected centers is listed, which when combined with systematic uncertainties gives the final measured value.

RMS $\lvert B\rvert$ (mG)	Fit center (Hz)	B shift (Hz)	Corrected center (Hz)
22	177 556 822±97	10±2	177 556 811±97
34	177 556 814±15	26±4	177 556 788±15
53	177 556 840±8	63±9	177 556 778±13
83	177 556 975±25	154±23	177 556 821±34
119	177 557 082±17	313±47	177 556 770±50
		Weighted average:	177 556 785±9
		dc Stark shift:	0±10
		Pressure shift:	0±20
		Power shift:	0±16
		Final measured value:	177 556 785±29

region, verifying that this effect is small. The average center for these two orientations is completely free of this reflection effect.

In a magnetic field, the $2S_{1/2}F=1m_F=0$ to $2S_{1/2}F=0m_F=0$ interval shifts quadratically at a rate [3] of 22.184 kHz/G^2, and the $2S_{1/2}F=1m_F=\pm1$ states shift linearly at a rate [3] of 1.3991 MHz/G. The measurement is done in magnetic fields which are small enough to make a precise measurement of the $2S_{1/2}F=1m_F=0$ to $2S_{1/2}F=0m_F=0$ interval but large enough to shift the $2S_{1/2}F=1m_F=\pm1$ to $2S_{1/2}F=0m_F=0$ resonances well away from the resonance to be measured. The magnetic fields used are 22, 34, 53, 83, and 119 mG in the vertical direction (this is the same direction as the 177.557-MHz rf magnetic field that drives the transition). It is advantageous to have little or no field in perpendicular directions so that $|\Delta m_F|=1$ transitions are not allowed, and thus off-vertical components are typically less than 10 mG. The magnetic fields are measured using a fluxgate magnetometer and a Gauss meter [11].

Table I shows the centers (averages of both directions of rf propagation and of both orientations of the rf region) for each of the five fields. When these centers are corrected for the expected quadratic shifts, they show excellent agreement.

Data are also taken at different background vacuum pressures. Typically the experiment is performed at pressures near 6×10^{-7} Torr, whereas on four occasions data are collected at approximately 25×10^{-7} Torr. Centers obtained at the high pressure are shifted by -78 ± 60 Hz with respect to the lower-pressure data. Assuming that there is a linear pressure shift, this would lead to a shift of 20 ± 15 Hz at our pressure of 6×10^{-7} Torr. Even though this does not give a strong indication of a pressure shift and even though we do not expect a pressure shift, we have included an uncertainty of 20 Hz due to pressure shift in Table I.

Data are also collected over a range of rf powers as a check for power shifts of the hyperfine interval. Most of our data are taken at 124 mW, but some are taken at 44, 75, and 182 mW. No shift versus power is expected, and the line centers obtained at these rf powers limits the possible linear power shift at 124 mW to 16 Hz, and this uncertainty is included in Table I.

The presence of dc electric fields also shift the resonance center. The shift rate is [3] $-(0.88E^2+0.23E_z^2)$ kHz/(V/cm)^2, where E is the magnitude of the electric field, and E_z is the vertical component of the electric field. To check for the presence of stray electric fields in the main rf region (due, for instance, to contact potentials or charging of surfaces), vertical electric fields ranging from $+1$ to -1 V/cm are added in this region by applying a voltage to the inner conductor of the region. This applied field quenches the metastable population by mixing $2S$ states with the short-lived $2P$ states. The quenching rate is found to be quadratic with applied electric field, and the fact that positive and negative applied fields give nearly the same quenching rate implies that the vertical component of the stray field is small ($E_z<0.018$ V/cm). A field of this size produces a shift of only 0.4 Hz. If the other components of the stray field are similarly small, the net shift on the resonance is negligible. Since it is unlikely that the other components would be much larger, we estimate that the net field is $E<0.09$ V/cm, and thus the shift is less than 10 Hz, as shown in Table I.

The MG3602A Anritsu signal generator used in this experiment receives its time base from a Stelar model 100B 10-MHz reference signal that is locked to the Global Positioning System and has a frequency stability of approximately 1×10^{-11}, leading to a negligible uncertainty in the measurement.

Overlap of other atomic resonances leads to negligible shifts of the resonance. The $2S_{1/2}F=1m_F=\pm1$ to $2S_{1/2}F=0m_F=0$ resonances are small (because the rf magnetic field is polarized in the vertical direction) and are far away (30–150 kHz away). The $2S$-to-$2P$ transitions are 1 and 10 GHz away. Possible contributions from longer-lived Rydberg states will be greatly reduced by the fact that the L's of high-n Rydberg states mix with the nP states in very small fields, and thus will be quenched in the electron bombardment region.

Table I gives the final measured value for the interval: 177 556 785±29 Hz, which is a 160-ppb measurement of the $2S$ hyperfine interval. The 29-Hz final uncertainty is a part in one hundred of the resonance linewidth. Given the careful studies of the systematic effects, and the present signal-to-noise ratio, splitting the line to a part in 100 is appropriate. To obtain a better measure of the line center, a better signal-to-noise ratio will be necessary.

The $2S$ hyperfine interval was first measured in Ref. [3] in 1956 to a precision of 280 ppb. These authors determined the interval to be 177 556 860±50 Hz, and this has remained the only measurement of the metastable hyperfine interval until the present work. Their measurement differs from ours by 75±58 Hz, indicating a modest disagreement between the two measurements.

The majority of contributions to the hyperfine structure of hydrogen scale as n^{-3}; however, there are a number of theoretical contributions that do not scale as n^{-3}. To isolate non-n^{-3} terms, the difference $D_{21}=8\nu_2-\nu_1$ is used, where ν_1 is the frequency of the $1S$ hyperfine interval and ν_2 is the frequency of the $2S$ hyperfine interval. The $1S$ interval was most recently measured by Essen *et al.* [1] to be $1\,420\,405\,751.7667\pm0.0001$ Hz, thus giving an experimentally determined value of $D_{21}=48\,528\pm232$ Hz. The uncertainty in D_{21} is entirely limited by the precision of the present $2S$ hyperfine measurement.

The three major theoretical [12] contributions to D_{21} are the Breit correction, the radiative corrections, and the nuclear-recoil correction. Fortunately, it was recently shown by Karshenboim [2] that nuclear structure-dependent corrections shift the difference D_{21} by 10^{-9} kHz. The theoretical prediction for D_{21} from Karshenboim [2] is $48\,942.66\pm0.01$ Hz. The difference between the experimental and theoretical determinations of D_{21} is -414 ± 232 Hz, which indicates a 1.8-standard-deviation discrepancy between theory and experiment. This discrepancy represents 0.8% of D_{21}.

In summary, the $2S_{1/2}F=1m_F=0$ to $2S_{1/2}F=0m_F=0$ interval in atomic hydrogen has been measured to be 177 556 785 Hz, with a one-standard-deviation uncertainty of ±29 Hz. This 160-ppb measurement is the most precise measurement of the $2S$ hyperfine interval to date. The measurement indicates that there may be additional theoretical contributions to D_{21} that have yet to be calculated.

This work was supported by the Natural Sciences and Engineering Research Council of Canada. The authors wish to acknowledge the work of Cody Storry during the initial stages of this measurement, as well as David Van Baak for lending us rf equipment and a palladium leak valve, and Steven Lundeen for use of his large-solid-angle Lyman-α detector.

[1] L. Essen *et al.*, Nature (London) **229**, 110 (1971).
[2] S. G. Karshenboim, Phys. Lett. A **225**, 97 (1997).
[3] J. W. Heberle, H. A. Reich, and P. Kusch, Phys. Rev. **101**, 612 (1956).
[4] J. Slevin and W. Stirling, Rev. Sci. Instrum. **52**, 1780 (1981).
[5] F. Biraben *et al.*, Rev. Sci. Instrum. **61**, 1468 (1990), M. Weitz, F. Schmidt-Kaler, and T. W. Hansch, Phys. Rev. Lett. **68**, 1120 (1992).
[6] W. W. Macalpine and R. O. Schildknecht, Proc. IRE **47**, 2099 (1959).
[7] J. T. M. Walraven and I. F. Silvera, Rev. Sci. Instrum. **53**, 1167 (1982).
[8] J. J. Bollinger and F. M. Pipkin, Rev. Sci. Instrum. **52**, 938 (1981); P. K. Majumder, Ph.D. thesis, Harvard, University, 1989.
[9] Norman F. Ramsey, *Molecular Beams* (Oxford University Press, Oxford, 1985).
[10] S. L. Palfrey, Ph.D. thesis, Harvard University, 1983.
[11] For more details on this and other systematic effects, see N. E. Rothery, Ph.D. thesis, York University, 1998.
[12] M. H. Prior and E. C. Wang, Phys. Rev. A **16**, 6 (1977).